

# A study on external CFRP reinforcement of precast concrete slabs with various cutout shapes

# **Tesfaye A. Mohammed** and **Azadeh Parvin**

Due to changes in structural or functional requirements, it may become necessary to introduce sectional openings in existing slabs of buildings and industrial facilities. Requirements for elevators, escalators, staircases, or utility ducts for heating and air-conditioning result in the creation of cutouts and removal of associated concrete and reinforcing steel bars. When part of a slab is removed, additional reinforcement is required to restore its ability to sustain imposed loads.

Fiber-reinforced polymer (FRP) composites provide an innovative way of strengthening precast concrete structural members because of their ease of installation, light weight, immunity to corrosion, high tensile strength, and availability in convenient forms. Few researchers have studied the structural response of slabs with openings. Vasques and Karbhari<sup>1</sup> investigated the effectiveness of externally bonded FRP strips for strengthening slabs with only one type of opening shape. They concluded that externally bonded FRP strips can be used to restore the original loadcarrying capacity of slabs weakened by cutouts. Enochsson et al.2 studied the amount of carbon-fiber-reinforced polymer (CFRP) sheets needed to restore the load-carrying capacity of slabs with cutouts to equal that of corresponding slabs without openings. Tan and Zhao<sup>3</sup> investigated the strengthening of openings in one-way slabs using CFRP sheets. They considered one type of opening shape with various dimensions located at the center of the slabs with the exception of one near the edges. They concluded that CFRP sheets can effectively enhance the load-carrying capacity and the stiffness of slabs with openings if prema-

### **Editor's quick points**

- Openings must sometimes be cut in slabs after construction to accommodate structural modifications for ducts, pipes, utilities, and elevators.
- In this study, slabs with rectangular and elliptical openings outperformed slabs with other opening shapes in terms of stiffness and ultimate flexural strength.
- CFRP strengthening enhanced the performance of all slabs with various openings by restoring the losses in stiffness and flexural strength caused by the openings.



ture failure due to FRP debonding is prevented. To the best of the authors' knowledge, there have been no studies on slabs with various opening shapes. In particular, investigations using finite element analysis (FEA), which takes into account material and geometrical nonlinearities of CFRP-strengthened precast concrete slabs with openings, are limited.

The present research contributes to the literature by proposing the development of reliable and complex nonlinear FEA models of as-built and CFRP-strengthened precast concrete slabs with various opening shapes. Circular, rectangular, elliptical, square, and diamond-shaped openings of equal area were considered to explore the effect of opening geometry on slab performance. The openings in the slabs were retrofitted with CFRP sheets around their perimeters to restore the original flexural strength and stiffness of the floors. The nonlinear FEA program ANSYS was used to model the slabs. A successful outcome for the proposed study would significantly reduce dependence on costly and time-consuming large-scale experimentation while maintaining a high degree of predictive capacity in capturing realistic characteristics of concrete slabs. The accuracy of the proposed FEA models was validated through experimental results reported in the literature by Tan and Zhao.<sup>3</sup> In the following sections the FEA modeling development, simulation results, and conclusions are discussed.

# Finite element analysis modeling of slabs

Element types, material models, geometry and mesh size, and boundary conditions were selected to develop the FEA models of the slabs.

### **Element types**

A three-dimensional (3-D) reinforced concrete element Solid65 was used to model the concrete. The Solid65 element is capable of cracking in tension and crushing in compression with options for large plastic deformation, nonlinear material property, and element death and birth attributes. It is defined by eight nodes and has three translational degrees of freedom at each node. Solid65 without reinforcing bars and with all mentioned attributes was used.

A 3-D spar element Link8 was employed to model all reinforcement bars. Link8 is a two-node, uniaxial, tension-compression element with three degrees of freedom at each node. Plasticity, creep, swelling, element death and birth, stress stiffening, and large deflection capabilities are the features of this element. The plasticity and element death and birth options were exercised.

To model CFRP sheets, the finite strain shell element Shell181 was employed. Shell181 is suitable for modeling thin to moderately thick shell structures with a membrane option. Again, plasticity, stress stiffening, large deflection, birth and death, and nonlinear stabilization are the features of this element. Shell181 is a four-node element with six degrees of freedom at each node, and it only has translational degrees of freedom with the membrane option. The birth and death and nonlinear stabilization options of this element were implemented in the development of FEA models.

### **Material models**

Concrete is a quasi-brittle material and has different behavior in compression and tension. A William-Warnke<sup>4</sup> material model with five input parameters was used as a failure criterion for the concrete. The uniaxial stress-strain curve for the concrete was defined according to the Desayi and Krishnan<sup>5</sup> and Gere and Timoshenko<sup>6</sup> equations. The compressive and tensile strengths of the concrete and the shear transfer coefficients  $\beta_t$  representing the conditions of the crack face were required as input data for ANSYS. The extreme  $\beta_t$  limits of 0 and 1 represent the absolute loss of shear transfer (smooth crack) and no loss of shear transfer (rough crack), respectively. Lower values of shear transfer coefficient induce convergence problems due to the sliding (shear) across the crack face, and therefore, smaller load increments should be used during the crack formation according to ANSYS instructions. The value of shear transfer coefficients reported in previous studies varied from 0.05 to 0.25.7,8 A preliminary analysis was conducted to calibrate the shear transfer coefficient values to avoid the convergence problem during the nonlinear analysis and to achieve a smooth shear transfer across the crack face. Shear transfer coefficient values of 0.02 for the open crack and 0.2 for the closed crack were found to be suitable for the numerical analysis.

The constitutive material properties of reinforcement bars were represented as an elastic-perfectly plastic material model and were assumed identical in tension and compression. The assumption of perfect bond between steel and concrete was enforced by connecting adjacent nodes of Link8 and Solid65 so that the two materials shared the same nodes.

The CFRP sheet was characterized as an orthotropic material model with options for fiber orientation layer. The assumption of perfect bond between the CFRP sheets and concrete was implemented by connecting adjacent nodes of Shell181 and Solid65 elements to share the same nodes.

# Mesh generation and boundary conditions

A preliminary analysis was conducted on the control slab model by varying the size of the mesh from coarse to fine and by comparing the deflection and compressive stress responses to identify a workable mesh density that would provide accurate results. Due to the symmetry, a quarter



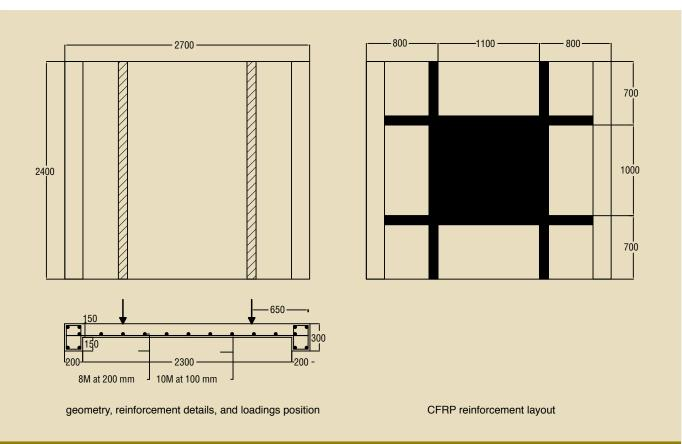


Figure 1. Lab details of the finite element validated model. Note: All measurements are in millimeters. CFRP = carbon-fiber-reinforced polymer. 1 mm = 0.0394 in.

of the slab was modeled to minimize computation time. The displacement in the direction perpendicular to the plane of symmetry was set to zero. To achieve even stress distributions and to avoid stress concentration, 30-mm-thick  $\times$  100-mm-wide (1.2 in.  $\times$  3.94 in.) and 30-mm-thick  $\times$  200-mm-wide (7.87 in.) steel plates were added at the locations of the applied loads and supports, respectively (**Fig. 1**). Three-dimensional Solid45 elements were used to model the steel plates. The slabs were simply supported.

## Nonlinear solutions and failure criterion

Death and birth options of each element were used to capture the post-peak behavior. The total load was applied in a series of load steps. An ANSYS parametric design language (APDL) macro code was used between load steps to identify the yielding of reinforcement elements and to deactivate (kill) adjacent concrete and CFRP elements to simulate the crushing of the concrete cover.

The Newton Raphson method option in ANSYS was used to satisfy the convergence at the end of each load increment within the tolerance convergence norms. The minimum and maximum load increments were controlled and predicted by ANSYS automatic load stepping based on the response of the structure for the previous load increment. In concrete cracking, reinforcement bar yielding, and post-peak phases,

a gradual small load increment was applied to capture the stiffness loss due to the crack propagation. As defined in the "Material models" section, the William-Warnke<sup>4</sup> failure criterion was used for the concrete material. The failure of the FEA slab model was recognized when the analysis stopped converging for a 0.001 kN (0.225 kip) load increment using APDL loading code.

# Finite element analysis results of validated models

Tan and Zhao<sup>3</sup> conducted an experimental study on CFRP-strengthened, one-way reinforced concrete slabs with openings. Using ANSYS program software, three of their test specimens—labeled RA1, RA2, and AS5—were used to validate the proposed FEA models. Specimens RA1 and RA2 were control reinforced-concrete slabs without and with openings, respectively. Specimen RA2's opening was 1100 mm long × 1000 mm wide (43.31 in. × 39.37 in.) and was located at the center of the slab. AS5 was the same as RA2, but it was strengthened by CFRP strips along the perimeter of the opening.

The concrete compressive strengths of specimens RA1, RA2, and AS5 were 41.2 MPa (5.98 ksi), 48.0 MPa (6.96 ksi), and 45.9 MPa (6.66 ksi), respectively. The Poisson's ratio of the concrete was assumed to be 0.2. The tensile strength and elastic modulus of concrete were calculated ac-



cording to ACI 318-05.9 Areas of longitudinal and transverse bars were 78.5 mm² (0.122 in.²) and 50.3 mm² (0.0780 in.²), respectively. Longitudinal reinforcement bars had a yield strength of 600 MPa (87.0 ksi) and elastic modulus of 165 GPa (23,900 ksi). Transverse reinforcement bars had a yield strength and elastic modulus of 640 MPa (92.8 ksi) and 175 GPa (25,400 ksi), respectively. The Poisson's ratio of reinforcement bars was assumed to be 0.3. **Figure 1** presents the geometry, reinforcement detailing, load configuration, and CFRP strip layout. The CFRP strips were 200 mm widex 1.2 mm thick (7.87 in. × 0.047 in.) with an elastic modulus of 165 GPa (23,900 ksi) and ultimate tensile strain of 1.7% along the unidirectional fibers.

The state of stiffness and flexural strength can be described by the load versus deflection curves. **Figure 2** compares the experimental and analytical results of specimens RA1, RA2, and AS5.

An immediate transfer of stresses from the concrete to the reinforcement bars was observed in the FEA results. The first crack occurred once the tensile strength of the concrete was reached. This phenomenon was witnessed in the load-deflection plots with a small horizontal plateau at the early loading stage. A large deflection was observed for a small load increment due to the first crack formation accompanied by the stiffness loss compared with the previous load step (**Fig. 2**).

The developed FEA models were able to capture the rapid change in the slope in the nonlinear portion of the load versus deflection curves beyond the first cracking stage, which was in agreement with the experimental results. Furthermore, the yielding of steel reinforcement bars was demonstrated with the formation of a plateau in the FEA load-deflection plots for specimens RA1 and RA2 as also reported in experimental results.

For the AS5 specimen, the internal reinforcement bars did not yield in the experiment or in the FEA slab model. This specimen failed by the CFRP strip debonding in the experiment as well as FEA as identified by the zigzag portion in the load versus deflection plots. The ultimate stage yielding plateau behavior was closely captured with the death and birth option of Solid65, Link8, and Shell181 elements used in the FEA.

FEA and experimental results were in agreement in all precracked, cracked, and ultimate stages for the RA1, RA2, and AS5 specimens. This validates the accuracy of the proposed FEA models for further parametric study.

### Case studies of as-built and strengthened precast concrete slabs with various opening shapes

Various case studies of as-built and CFRP-strengthened precast concrete slabs were investigated using the validated

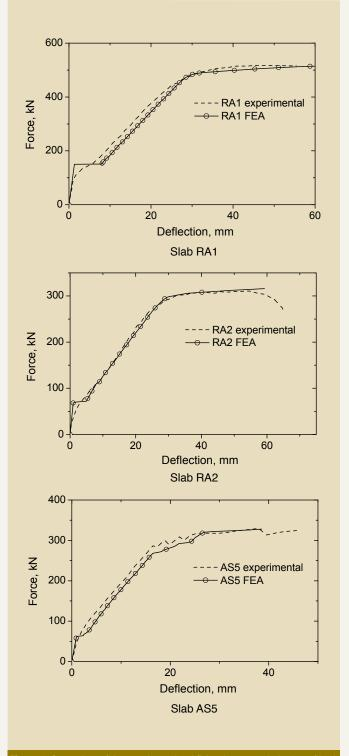


**Figure 2.** Comparison of the experimental and finite element analysis plots of load versus deflection. Note: 1 mm = 0.0394 in.; 1 kN = 0.225 kip.

FEA models and techniques to optimize the opening shapes for the minimum amount of losses in the stiffness and the flexural strength caused by the cutout in the slabs. The slab opening shapes considered were circular, diamond, elliptical, rectangular, and square with equal areas. **Figure 3** shows dimensions, locations, and geometries of the openings. Slab dimensions, steel reinforcement details and properties, and boundary conditions were identical to the vali-



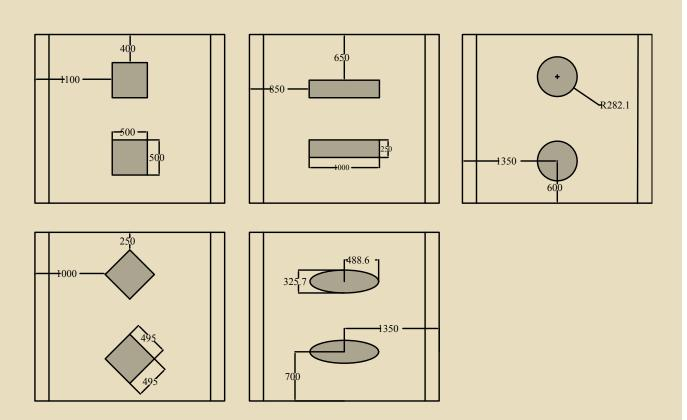


Figure 3. Locations, geometries, and dimensions of the openings studied. Note: All measurements are in millimeters. 1  $\underline{mm} = 0.0394$  in.

dated models for all case studies. The concrete compressive strength was 40.0 MPa (5.8 ksi). **Table 1** shows the material properties of the CFRP sheets. The CFRP sheets consisted of one layer of unidirectional fiber and had a 200 mm (7.87 in.) width in all strengthened case studies. The main focus of the present study was on the various shapes of the opening for the slab while keeping the effect of other variables constant. For this reason the total area of openings, the amount of the CFRP reinforcements, and the layouts were similar for all case studies. Additional diagonal CFRP sheet reinforcements were not provided for shapes with sharp edges. **Figure 4** shows the CFRP sheet layouts.

# As-built precast concrete slabs with various opening shapes FEA results

Load versus deflection curves in Fig. 5 demonstrate the

characteristics of as-built precast concrete slabs with and without various opening shapes. The as-built precast concrete slab with rectangular openings exhibited the least amount of stiffness and flexural strength losses. The as-built precast concrete slabs with rectangular, elliptical, square, circular, and diamond-shaped openings lost 15.7%, 38.7%, 41.6%, 48%, and 51.6% of ultimate load-carrying capacity compared with the solid precast concrete slab.

The slope of the load versus deflection curve represents the stiffness of the precast concrete slab at a certain loading level. In this study, the mean stiffness values were reported after the first crack-formation stage as each slab exhibited identical linear behavior up to the cracking load. As-built precast concrete slabs with square and elliptical openings had comparable losses of stiffness. Overall, the slabs with circular- and diamond-shaped openings exhibited the high-

**Table 1.** Properties of the carbon-fiber-reinforced polymer sheets

Properties	ASTM method	Test value	Design value
Ultimate tensile strength	D-3039	986 MPa	834 MPa
Ultimate elongation	D-3039	1%	1%
Tensile modulus	D-3039	95.8 GPa	82 GPa
Laminate thickness per ply	n.d.	1.0 mm	1.0 mm

Note: n.d. = no data. 1 mm = 0.0394 in.; 1 MPa = 0.145 ksi; 1 GPa = 145 ksi.



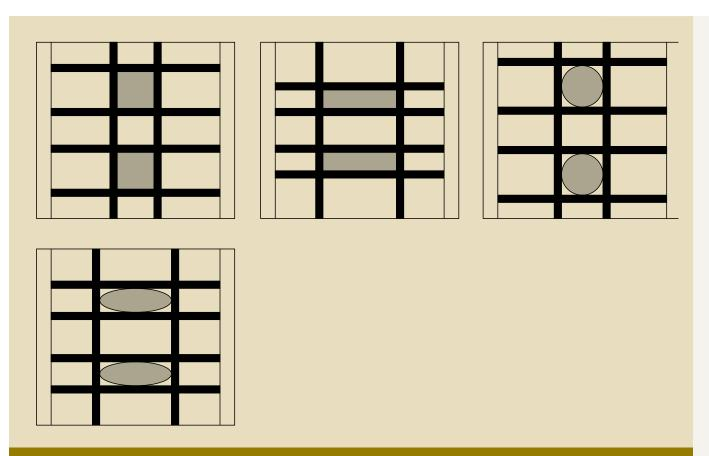


Figure 4. CFRP reinforcement layout for the differently shaped openings.

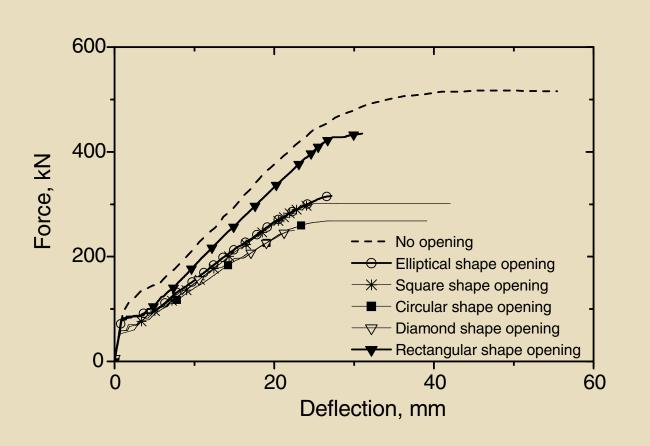


Figure 5. The load-deflection plots of as-built slabs with various opening shapes. Note: 1 mm = 0.0394 in.; 1 kN = 0.225 kip.



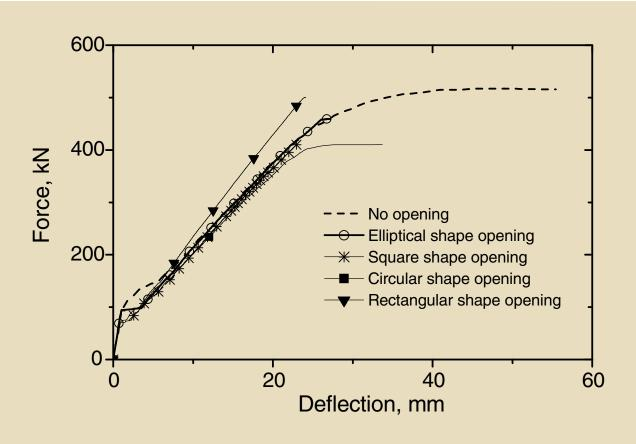


Figure 6. Load-deflection plots of strengthened slabs with various opening shapes. Note: 1 mm = 0.0394 in.; 1 kN = 0.225 kip.

est stiffness loss (34.4%) compared with the solid precast concrete slab. This loss of stiffness became more apparent as the loading continued beyond the first crack formation. The slab with diamond-shaped openings was not used in the subsequent investigation of the CFRP-strengthened slabs. This was due to the poor structural performance and numerical instability in the FEA of strengthened precast concrete slab with diamond-shaped openings.

# FEA results of CFRP-strengthened precast concrete slabs with various opening shapes

**Figure 6** shows the load versus deflection curves of retrofitted slabs. Similar to as-built case studies, the studies of strengthened precast concrete slab showed that rectangular openings outperformed other opening shapes in terms of gains in stiffness and flexural strength. These gains became more apparent as the loading continued beyond the first crack. The CFRP-strengthened precast concrete slab with rectangular openings sustained a similar level of maximum ultimate load and a 26% increase in the maximum stiffness compared with the solid precast concrete slab.

The CFRP-strengthened precast concrete slabs with square and circular openings attained lower ultimate loads compared with the solid slab. The specimen with ellipti-

cal openings restored its original stiffness but lost 11% of the original ultimate load-carrying capacity. In terms of deflection, the solid slab followed by the slab with circular openings had the largest values. In contrast to the ductile failure type observed in the solid precast concrete slab, all CFRP-strengthened precast concrete slabs with openings had brittle failure with the exception of those with circular openings. Similar behaviors were witnessed in the experimental study of the CFRP-strengthened slab with a rectangular opening (AS5), which was used to validate the accuracy of the proposed FEA models.

### Stress contours

A cutout in the slab causes disturbance in the transfer of stresses. The stress level and distribution around the edges and corners depend on the shape and dimensions of the opening. Stress contours were plotted to examine the stress gradients near and around the openings. **Figure 7** shows top concrete surface stress distributions of the CFRP-strengthened precast concrete slabs with various opening shapes. The light colors represent lower stress values, such as negative compressive stress values. The dark colors represent higher stress values, such as positive tensile stress values.

Irregular gradient stress distributions were observed in





**Figure 7.** Stress contours taken from quarter-slab models having various opening shapes.

strengthened precast concrete slabs adjacent to square, circular, and elliptical openings. Relatively uniform gradient stress distributions were observed near rectangular openings. This phenomenon was attributed to the higher aspect ratio of the rectangular openings compared with other slab openings. The uniform gradient stress distributions mitigated the formation of stress concentrations around the opening edges and enhanced the structural performance of strengthened precast concrete slab with rectangular openings. In all of the plots, uneven stress gradients were observed at the applied load locations.

### Conclusion

The FEA has shown that CFRP strengthening is effective in restoring and even enhancing the structural performance of precast concrete slabs with openings. The FEA results demonstrated that rectangular openings outperformed other opening shapes with minimum loss of stiffness, flexural strength, and ultimate load-carrying capacity. All CFRP-

strengthened precast concrete slabs with openings exhibited brittle failure except the slab with circular openings.

### **Acknowledgments**

This work was supported in part by an allocation of computing time from the Ohio Supercomputer Center.

### References

- Vasques, A., and V. M. Karbhari. 2003. Fiber Reinforced Polymer Composite Strengthening of Concrete Slabs with Cutouts. *ACI Structural Journal*, V. 100, No. 5 (September–October): pp. 665–673.
- Enochsson, O., J. Lundqvist, B. Taljsten, P. Rusinowski, and T. Olofsson. 2007. CFRP Strengthened Openings in Two Way Concrete Slabs—An Experimental and Numerical Study. *Journal of Construction Building Materials*, V. 21, No. 4 (April): pp. 810–826.

- H H H H -C-C-C-C-H H H H
- Tan, K. H., and H. Zhao. 2004. Strengthening of Openings in One-Way Reinforced Concrete Slabs Using Carbon Fiber Reinforced Polymer Systems. ASCE Journal of Composites for Construction, V. 8, No. 5 (September–October): pp. 393–402.
- 4. Willam, K. J., and E. D. Warnke. 1975. Constitutive Model for Triaxial Behavior of Concrete. *Proceedings of the International Association for Bridge and Structural Engineering*, V. 19. Bergamo, Italy.
- 5. Desayi, P., and S. Krishnan. 1964. Equation for the Stress-Strain Curve of Concrete. *Journal of the American Concrete Institute*, V. 61, No. 3 (March): pp. 345–350.
- 6. Gere, J. M., and S. P. Timoshenko. 1997. *Mechanics of Materials*. Boston, MA: PWS Publishing Co.
- 7. Bangash, M. Y. H. 1989. *Concrete and Concrete Structures: Numerical Modeling and Applications*. London, England: Elsevier Science Publishers Ltd.
- 8. Hemmaty, Y. 1998. Modeling of the Shear Force Transferred Between Cracks in Reinforced and Fibre Reinforced Concrete Structures. In *Proceedings of the ANSYS Conference*, V. 1, Pittsburgh, PA.
- 9. American Concrete Institute (ACI) Committee 318. 2005. *Building Code Requirements for Reinforced Concrete (ACI 318-05) and Commentary (318R-05)*. Farmington Hills, MI: ACI.

### **Notation**

 $\beta_t$  = shear transfer coefficients



### **About the authors**



Tesfaye A. Mohammed is a PhD student in the Department of Civil Engineering at the University of Toledo in Toledo, Ohio.



Azadeh Parvin, DSc, is an associate professor in the Department of Civil Engineering at the University of Toledo.

### **Synopsis**

In some cases, openings must be introduced after slab construction to accommodate ducts, pipes, utilities, and elevators. This study involves the development of three-dimensional, complex, nonlinear finite element analysis (FEA) models of precast concrete slabs with and without openings. One solid precast concrete slab and five slabs with various opening shapes but equal areas were considered. The openings in the slabs were retrofitted with carbon-fiber-reinforced polymer (CFRP) sheets around their perimeters to restore the original flexural strength and stiffness of the floors. Rectangular, circular, square, elliptical, diamond-shaped openings were investigated for the control specimens and the corresponding CFRP-strengthened slab models. An experimental study on a reinforced

concrete solid slab and as-built and CFRP-strengthened slabs with rectangular openings reported in the literature was used to validate the accuracy of the proposed FEA models. The FEA results revealed that the slabs with rectangular and elliptical openings outperformed the slabs with other opening shapes in terms of stiffness and ultimate-flexural-strength capacity. CFRP strengthening enhanced the performance of all of the slabs with openings compared with their corresponding control models. Through CFRP reinforcement, the losses in stiffness and flexural strength caused by the cutouts were restored. In the case of the slab with rectangular openings, similar flexural strength and increased stiffness were attained compared with the slab without any opening.

### Keywords

Carbon-fiber-reinforced polymer, CFRP, finite element analysis, FEA, opening, slab.

### **Review policy**

This paper was reviewed in accordance with the Precast/Prestressed Concrete Institute's peer-review process.

### Reader comments

Please address any reader comments to journal@pci. org or Precast/Prestressed Concrete Institute, c/o *PCI Journal*, 200 W. Adams St., Suite 2100, Chicago, IL 60606.